An MTL-based Channel Model for Indoor Broadband MIMO Power Line Communications

Julio A. Corchado, José A. Cortés, Francisco J. Cañete and Luis Díez

***Abstract*—The recent release of indoor Power Line Communications (PLC) standards with Multiple-Input Multiple-Output (MIMO) capabilities has arisen the need for channel models that reflect the multiconductor nature of the grid. This paper proposes a model, based on the multiconductor transmission line (MTL) theory, along with a random PLC channel generator operating in the frequency range from 1 to 100 MHz. Its distinctive features are the modeling of three key elements: the asymmetry in the layout caused by the derivations to the light switches, the impedance of the devices connected to the three wires of the grid and the variable distance between conductors in loose wiring deployments. The influence of these elements in the spatial correlation between the streams of the MIMO links is studied and compared with measurements.**

***Index Terms*—Power line communications, multiple-input multiple-output, broadband, spatial correlation, multiconductor transmission line, channel modeling**

I. Introduction

Power Line Communication consists in the exchange of information over electrical cables. PLC takes advantage of the ubiquity of already deployed power delivery networks and provides access to telecommunication services without any further infrastructure installation. Recently, PLC has emerged as a true contender in the domestic broadband communication technologies, a field which has been controlled by wireless-based solutions for many years.

The indoor electrical network is well suited for power delivery (50-60 Hz signal) but presents unfriendly behavior for high frequency signals, which demands tools capable of modeling these scenarios' features. However, the uncertainties in the network topology and in the response of electrical appliances make channel modeling a challenging task. Since most modern power grids have three conductors: phase, neutral and protective earth; wired MIMO schemes can be adopted by using differential transmission among them. Actually, there already exist standards that cover MIMO capabilities for in-home PLC schemes [1], [2].

The modeling of MIMO PLC channels has been addressed by extending the two approaches developed for SISO (Single-Input Single-Output) ones, which are commonly referred to as top-down and bottom-up. In the former, the channel response is represented by a sum of delayed echoes whose parameters are derived from measurements [3]. In the latter, channels are obtained from a model of the physical structure of the power grid [4].

J. A. Corchado, F. J. Cañete and L. Díez (julioalc, francis, diez@ic.uma.es) are with the Departamento de Ingeniería de Comuniaciones, Escuela Técnica Superior de Ingeniería de Telecomunicación, Universidad de Málaga, Spain.

José A. Cortés (jaca@ic.uma.es) is a consultant in Málaga, Spain.

The top-down strategy is computationally simpler than the bottom-up. However, obtaining a set of parameters that yields a good fitting to actual channels requires a large number of measurements. In fact, due to the great dispersion of the channel response characteristics (even within the same indoor network), channels are usually classified into categories that are fitted using a different set of model parameters [5]. As an example, a classification into 4 categories was proposed in [6], which was proved to be insufficient in [7]. Later works extended this figure up to 9 categories [8].

The MIMO extension of the top-down strategy is achieved by including a term that models the correlation between the SISO streams. As it will be shown in this work, this correlation depends on the type of cabling, the topology of the power grid and the devices connected to it. Since these elements vary significantly among indoor networks, measurements used to compute the aforementioned model parameter should be also classified into categories in which the fitting process should be performed independently. The combination of these categories with the ones employed to match the characteristics of the SISO streams results in a very large number of sets. In contrast, studies published up to now employ measurements carried out in a few number of scenarios. Hence, they do not consider channel categorization at all [9], or it is only applied to the channels generated according to the proposed model, which are then individually fitted to the same set of measured channels [10].

The bottom-up strategy is based on a description of the physical topology of the power grid, which is modeled using the transmission line theory. Both the two-conductor and the multiconductor line theory (MTL) have been employed to model SISO channels [4], [11], [12]; but only MTL can be used in the MIMO case [13]. Bottom-up models are particularly useful for multicast studies, since they naturally reflect the correlation among the channels of a given site that share a common communication end point [14], [15]. This feature also makes bottom-up models specially suitable for simulating multihop PLC transmission strategies, e.g. amplify-and-forward (AF) and decode-and-forward (DF) relaying, single-frequency networks (SFN) and distributed space-time coding. Accordingly, most published works related to this field use the bottom-up channel modeling strategy [16]–[18]. Bottom-up models are also useful for coverage predictions, where the response of the channels established in a particular scenario has to be estimated only from the power grid description, without accomplishing measurements. This need arises in applications where PLC technology is used in large environments, for instance, to serve as the backhaul of wireless access points deployed in train stations and airports [19]. Bottom-up models

can be also employed to obtain statistically representative channels by generating topologies in a random manner [11], [20]. For the latter, top-down models are computationally simpler (their computational burden resides in the calculation of the model parameters). Hence, the most suitable modeling technique for SISO channels depends on the application.

However, bottom-up MIMO models are particularly interesting because of a twofold reason. First, because of the complexity of the measuring process [21], which makes difficult the acquisition of sets of measurements that cover the wide range of indoor networks characteristics, e.g., power grid size, type of cabling and type of connected devices. Second, because the lack of knowledge about the influence of the aforesaid elements in the correlation between the SISO streams may lead to a biased selection of the channels employed to derive the corresponding parameter of the top-down model.

From now on, the term spatial correlation will be used to denote the relation between the SISO streams that form a MIMO channel. The condition number of the channel matrix (the ratio of the largest eigenvalue to the lowest one) is the conventional way to characterize such relation [22].

In this context, the present work makes four contributions:

- It gives a statistical analysis of the correlation between the SISO streams of 120 measured 2x2 MIMO channels. These results are compared to the ones obtained with channels generated with a plain MTL-based model. It will be shown that, while modelled links exhibit the same correlation value at all frequencies (measured in terms of the ratio between the singular values), significant variations occur in the measured ones.
- It identifies that plain MTL-based models are unable to reflect the correlation of actual channels because they disregard all the asymmetries existing in indoor power grids. Of particular importance are the ones concerned with the layout, the input impedance of three-pin plug devices connected to the network and, when unipolar cables are employed, the variable distance between them.
- It proposes an MTL-based model, and an associated channel generator, that incorporates the aforementioned asymmetries. It also allows generating statistically representative channels by means of a random topology generator that complies with the deployment practices used in most European countries. The suitability of the proposed model to reflect both the characteristics of the individual SISO streams and the correlation between them is assessed by comparing an ensemble of generated MIMO channels to the set of 120 measured ones.
- It highlights the influence of several elements of indoor power grids in the spatial correlation of MIMO channels. Provided considerations can be helpful to categorize indoor networks into classes in which the fitting of top-down models should be accomplished independently.

The rest of this paper is organized as follows. Section II provides some background on the in-home electric grid. In Section III, we present the theoretical analysis of the three conductor transmission line configuration based on MTL equations. In section IV, a model for the in-home MIMO PLC channel featuring is introduced, from which a MIMO PLC channel generator is derived in section V. The proposed model is validated in Section VI. Presented results are also used in Section VII to discuss the influence of some indoor power grid elements on the spatial correlation. Finally, conclusions are given in Section VIII.

II. The indoor power grid

In this section, some insight into the in-home power grid is provided in order to support the modeling decisions that will be taken later on. In-home PLC channels vary greatly from one location to another. Although most buildings have the already mentioned three-conductor power grid, the way the multiconductor wiring is deployed varies among countries (grounding practices, monopolar/multipolar wiring, etc.) and this leads to significant differences in some MIMO properties.

For the purpose of this document, we define the indoor power grid as the wiring between the main panel and the network ending points (wall sockets and lighting circuit ends). The grid is split in a number of sub-circuits which are connected to the main panel and then each sub-circuit divides itself into several branches which cover the place. Small indoor power grids, like those found in little houses and apartments, usually have five sub-circuits; three of these sub-circuits provide electricity to low-power devices; while the rest of the sub-circuits feed high power devices, such as water heaters and ovens. The structure of an indoor power grid resembles a tree where the main panel is the root, the sub-circuits are the main branches and the wall sockets and devices connected to it are the leaves. An example of this structure is shown in Figure 1. Wall sockets are used as modem entrances to the network and belong often to the low-power sub-circuits, usually the ones with the largest number of branches. In indoor PLC the biggest issue is the large number of branches that form the power grid. These branches lead to discontinuities which bring a large number of signal reflections, causing problems due to multipath effects and energy dispersion. On the other hand, path length is not as important as it is in outdoor PLC, due to the fact that these distances are usually within tens of meters whereas connections of hundreds of meters are common in outdoor PLC.

The other indoor power grid elements that will be discussed are the network ending points, which are classified either as devices or empty sockets. These elements would play the role of the tree leaves depicted in Figure 1. It will be assumed that all three conductors reach every single ending point, although sometimes there are sockets that only show two conductors. Regarding the characterization of the devices impedance, in [4] and [23] it can be seen that the impedance values they present to the network vary greatly depending on the type of device we are dealing with. However, only the response between a single pair of conductors (e.g. phase and neutral) is measured and, thus, the third conductor (protective earth) is not taken into account. According to measurements performed by our own on some devices, it is needed to take into account the three conductors to properly capture the impedance that these elements show.

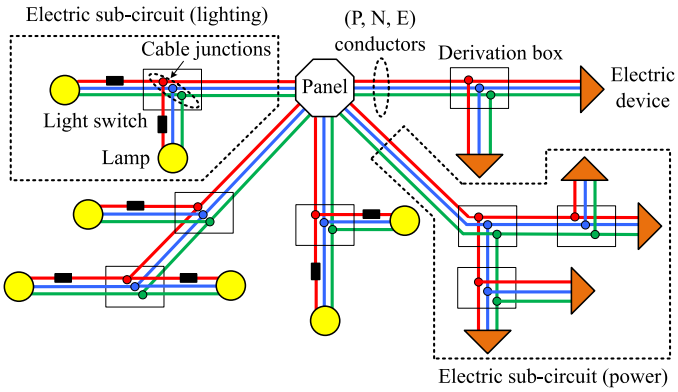

Fig. 1. Tree structure for the indoor power grid. Five sub-circuits hang from the main panel: three lighting circuits, with light switches derivations and lighting/socket terminations (yellow circles); two power-delivery circuits, ended in high power consumption appliances (orange triangles).

III. MTL FRAMEWORK

We herein describe the framework used in the modeling of MIMO indoor power-line channels. It is largely based on the well-established MTL theory [24], but has been included for the sake of completeness. We first report the fundamental MTL relations and we summarize the expressions used to derive the per unit length (p.u.l.) parameter matrices. Then, we propose a procedure for the computation of the MIMO Channel Frequency Response (CFR) between any pair of nodes in power line networks that deploy multiconductor lines. The method is based on the division of the channel in a number of segments which can be characterized by transmission matrices, an approach similar to that already employed in [13]. The product of these transmission matrices belonging to their respective channel segments form the complete channel transmission matrix from which the CFR can be derived.

A. MTL equations

The idea behind MIMO signal transmission in PLC networks consists in the use of three wires: Phase (P), Neutral (N) and Protective Earth (E). Coupling effects provide interactions between them, therefore, by transmitting and receiving over two pairs of wires, a 2×2 MIMO system is defined. The use of multidimensional p.u.l. parameters is required to capture the nature of these interactions between P, N and E.

In indoor PLC, the transversal dimension of the cable structure is relatively small with respect to the transmission signal wavelength in the considered frequency range (i.e. under 100 MHz) and we can make the TEM (Transverse ElectroMagnetic) or quasi-TEM propagation mode assumption which, along with the uniform dielectric assumption, allows the use of uncomplicated expressions for the p.u.l. parameter matrices.

Now, let $V_k(f,x)$ be the voltage phasor, at frequency f and coordinate x, associated to the circuit which comprises conductor k and the reference one. For simplicity, from now on we will just use $V_k(x)$, omitting the frequency dependence.

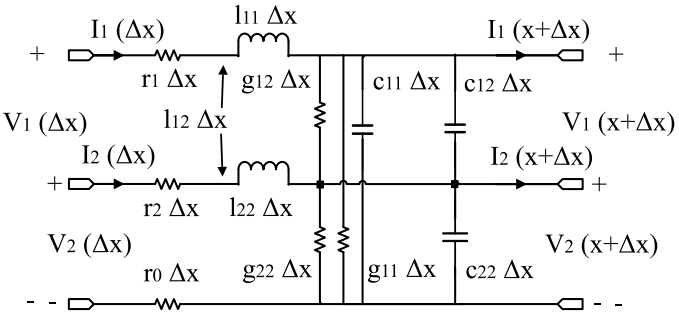

Fig. 2. Model for the per-unit-length parameters of the three conductor line.

The telegrapher's equations in the frequency domain can be obtained by letting $\Delta x \to 0$ in Fig. 2:

$$\frac{\partial \mathbf{V}(x)}{\partial x} = -(\mathbf{R} + j2\pi f \mathbf{L})\mathbf{I}(x) \tag{1}$$

$$\frac{\partial \mathbf{I}(x)}{\partial x} = -(\mathbf{G} + j2\pi f \mathbf{C})\mathbf{V}(x) \tag{2}$$

where $\mathbf{V} = [V_1, V_2]^T$ is the voltage phasor vector, $\mathbf{I} = [I_1, I_2]^T$ is the current phasor vector and $(-)^T$ denotes the transpose operator.

Moreover

$$\mathbf{R} = \begin{bmatrix} r_1 + r_0 & r_0 \\ r_0 & r_2 + r_0 \end{bmatrix}, \mathbf{C} = \begin{bmatrix} c_{11} + c_{12} & -c_{12} \\ -c_{12} & c_{22} + c_{12} \end{bmatrix} \tag{3}$$

$$\mathbf{G} = \begin{bmatrix} g_{11} + g_{12} & -g_{12} \\ -g_{12} & g_{22} + g_{12} \end{bmatrix}, \mathbf{L} = \begin{bmatrix} l_{11} & l_{12} \\ l_{12} & l_{22} \end{bmatrix} \tag{4}$$

are the p.u.l. parameter matrices for the resistance, capacitance, conductance and inductance, according to Fig. 2 [24].

The MTL equations can then be obtained by means of a first derivative and a substitution

$$\frac{\partial^2 \mathbf{V}(x)}{\partial x^2} = \mathbf{ZY}\mathbf{V}(x) \tag{5}$$

$$\frac{\partial^2 \mathbf{I}(x)}{\partial x^2} = \mathbf{YZ}\mathbf{I}(x) \tag{6}$$

where $\mathbf{Z} = \mathbf{R} + j2\pi f \mathbf{L}$ and $\mathbf{Y} = \mathbf{G} + j2\pi f \mathbf{C}$ are defined as the impedance and admittance matrix, respectively.

It can be shown that by means of a similarity transformation [24], one can solve the phasor MTL equations to obtain the transmission parameter matrix, $\mathbf{\Phi}$, of any transmission line with length L given its p.u.l. parameter matrices. Matrix $\mathbf{\Phi}$ is defined as follows

$$\begin{bmatrix} \mathrm{V}_1^{\mathrm{out}} \\ \mathrm{V}_2^{\mathrm{out}} \\ \mathrm{I}_1^{\mathrm{out}} \\ \mathrm{I}_2^{\mathrm{out}} \end{bmatrix} = \mathbf{\Phi} \begin{bmatrix} \mathrm{V}_1^{\mathrm{in}} \\ \mathrm{V}_2^{\mathrm{in}} \\ \mathrm{I}_1^{\mathrm{in}} \\ \mathrm{I}_2^{\mathrm{in}} \end{bmatrix} \tag{7}$$

while currents $\mathrm{I}_i^{\mathrm{in/out}}$ and voltages $\mathrm{V}_i^{\mathrm{in/out}}$ are depicted in Figure 3.

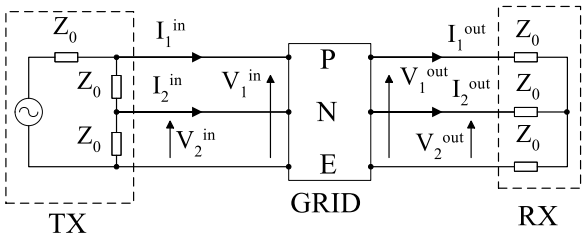

Fig. 3. Lumped element model for both transmitter (left) and receiver (right) ends. The transmitter configuration corresponds to a signal injection between protective earth and phase conductors (E-P). Transmitter and receiver impedance values are all set to $Z_0 = 50\ \Omega$.

The submatrices of $\mathbf{\Phi}$ are given by:

$$\begin{aligned}
\mathbf{\Phi_{11}} &= \frac{1}{2}\mathbf{Y}^{-1}\mathbf{T}\left(e^{\mathbf{\Gamma}L} + e^{-\mathbf{\Gamma}L}\right)\mathbf{T}^{-1}\mathbf{Y} \\
\mathbf{\Phi_{12}} &= -\frac{1}{2}\mathbf{Z_C}\left[\mathbf{T}\left(e^{\mathbf{\Gamma}L} - e^{-\mathbf{\Gamma}L}\right)\mathbf{T}^{-1}\right] \\
\mathbf{\Phi_{21}} &= -\frac{1}{2}\left[\mathbf{T}\left(e^{\mathbf{\Gamma}L} - e^{-\mathbf{\Gamma}L}\right)\mathbf{T}^{-1}\right]\mathbf{Y_C} \\
\mathbf{\Phi_{22}} &= \frac{1}{2}\mathbf{T}\left(e^{\mathbf{\Gamma}L} + e^{-\mathbf{\Gamma}L}\right)\mathbf{T}^{-1}
\end{aligned} \tag{8}$$

where the matrices $\mathbf{T}$ and $\mathbf{\Gamma}$ result from the diagonalization process

$$\sqrt{\mathbf{YZ}} = \mathbf{T\Gamma T}^{-1}, \tag{9}$$

the characteristic impedance matrix, $\mathbf{Z_C} = {\mathbf{Y_C}}^{-1}$, is defined as

$$\mathbf{Z_C} = \mathbf{Y}^{-1}\mathbf{T\Gamma T}^{-1} \tag{10}$$

and the matrix exponential follows

$$e^{\mathbf{\Gamma}L} = \begin{bmatrix} e^{\Gamma_1 L} & 0 & \dots & 0 \\ 0 & e^{\Gamma_2 L} & \ddots & \vdots \\ \vdots & \ddots & \ddots & 0 \\ 0 & \dots & 0 & e^{\Gamma_N L} \end{bmatrix} \tag{11}$$

with $\mathbf{\Gamma} = diag(\Gamma_1, \Gamma_2, \dots, \Gamma_N)$.

B. Transmission matrix approach

The goal of this section is to compute the MIMO CFR between any pair of nodes in power line networks that comprise multiconductor lines and several branches and loads. We propose computing the CFR by splitting the channel into manageable parts, characterizing each one by its transmission matrix [25], obtaining the global transmission matrix as the product of all these partial matrices and from there computing the global CFR. We first reorganize the MTL network into a main path and a set of branches that depart from intermediate nodes of the main path. The main path is the shortest signal path between the transmitter and the receiver. Thus, the resultant scenario consists of a set of secondary branches put in between the main path lines.

The equations for the transmission matrix of a transmission line have been shown in (8), and can be used to characterize those secondary branches. Let, without any loss of generality, the secondary branch be a line of length L terminated in any load with admittance matrix $\mathbf{Y_{br}}$. The input impedance seen from the main path can be computed as

$$\mathbf{Z_{input}} = -\left(\mathbf{\Phi_{11}} - \mathbf{\Phi_{12}}\mathbf{Y_{br}}\right)\left(\mathbf{\Phi_{21}} - \mathbf{\Phi_{22}}\mathbf{Y_{br}}\right)^{-1}. \tag{12}$$

Once we have obtained $\mathbf{Z_{input}}$, the transmission parameter matrix of the secondary branch can be computed with the following expressions

$$\begin{aligned}
\mathbf{\Phi_{11}} &= \mathbf{\Phi_{22}} = \mathbf{1}_n \\
\mathbf{\Phi_{12}} &= \mathbf{0}_n \\
\mathbf{\Phi_{21}} &= -{\mathbf{Z_{input}}}^{-1}
\end{aligned} \tag{13}$$

where $\mathbf{1}_n$ is the $n \times n$ identity matrix and $\mathbf{0}_n$ is a $n \times n$ zero matrix.

Then the transmission parameter matrix for the whole channel, $\mathbf{\Phi^{Total}}$, is:

$$\mathbf{\Phi^{Total}} = \mathbf{\Phi^{[n]}} \times \mathbf{\Phi^{[n-1]}} \times \dots \times \mathbf{\Phi^{[2]}} \times \mathbf{\Phi^{[1]}} \tag{14}$$

where $\mathbf{\Phi^{[m]}}$ is the transmission parameter matrix of the m-th segment.

Now, we can obtain the transmission matrix of the equivalent two-port system ϕ^{ij}, between the pair of conductors $i - ref$ at input and the pair of conductors $j - ref$ at output, from the $(n+1)$-port circuit with

$$\begin{aligned}
\phi_{11}^{ij} &= -\mathbf{\Upsilon}^{-1}(j,:)\mathbf{\Phi^{Total}}(:,i) \\
\phi_{12}^{ij} &= -\mathbf{\Upsilon}^{-1}(j,:)\mathbf{\Phi^{Total}}(:,n+i) \\
\phi_{21}^{ij} &= -\mathbf{\Upsilon}^{-1}(n+1,:)\mathbf{\Phi^{Total}}(:,i) \\
\phi_{22}^{ij} &= -\mathbf{\Upsilon}^{-1}(n+1,:)\mathbf{\Phi^{Total}}(:,n+i)
\end{aligned} \tag{15}$$

where the matrix $\mathbf{\Upsilon}$ is given by

$$\begin{aligned}
\mathbf{\Upsilon}(1:n, 1:n) &= -\mathbf{1}_n \\
\mathbf{\Upsilon}(n+1:2n, 1:n) &= \mathbf{0}_n \\
\mathbf{\Upsilon}(:, n+2:2n) &= \mathbf{\Phi}^{Total}(:, [1, \dots, i-1, i+1, \dots, n]) \\
\mathbf{\Upsilon}(n+1, n+1) &= 0 \\
\mathbf{\Upsilon}(n+j, n+1) &= -1
\end{aligned} \tag{16}$$

Finally, the CFR between the chosen ports is given by

$$H^{ij} = \phi_{11}^{ij} - \frac{\phi_{12}^{ij}\phi_{21}^{ij}}{\phi_{22}^{ij}}. \tag{17}$$

Therefore, the $n \times n$ MIMO matrix, $\mathbf{H}$, can be formed by getting the CFR of all existing port connections.

IV. The MIMO channel model

As pointed out in section II, the in-home power grid follows a tree-like structure that can be modeled with nodes (main panel, network ends and intersections) and branches (segments of wiring). The approach presented here to MIMO PLC channel modeling is somehow similar to the works presented in [12] (SISO) and [26] (MIMO). Thus, for the sake of conciseness, in this section we will only define the novel elements of our proposal, which will be classified in three different categories: cabling, branches and loads.

Fig. 4. Cross section of typical cables used in in-home power grids: multipolar ribbon (left), multipolar symmetric (center) and monopolar (right). The dashed circumference represents the ribbed plastic tube where in-home cabling is usually enclosed in.

A. Cabling

It has been found that the kind of wiring deployed in the indoor power grid strongly influences the spatial correlation between the streams of the MIMO links. Channels whose wires have fixed distances between conductors, either because of the use of multipolar cables or very tight conduits, present an approximately constant spatial correlation which translates to a roughly invariant value of the condition number of the MIMO channel matrix. Moreover, even when monopolar cables are used, a common assumption is that all three wires are deployed in a parallel fashion with the same spacing between them. This practice is caused by the uncertainty about how wires are deployed inside the conduit and also because it is the simplest approach. These premises do not hold for most cases, although the parallel wire assumption is needed in order to apply the analytic expressions for the computation of the p.u.l. parameter matrices (3) and (4).

In order to better reflect the spatial correlation that exists in indoor grids where monopolar cables are loosely deployed, while fulfilling the necessary conditions required to compute the p.u.l. parameters, the following approach is proposed: first of all, it is assumed that all three wires belonging to the same sub-circuit of the grid have always the same diameter; all lines are split into five segments, each one with its own spacing between conductors. There is a trade-off between spatial correlation and network complexity when setting the number of segments we split each line into; simulations showed that five segments provide enough spatial correlation while keeping the number of elements in the model reasonably low. It will be shown that monopolar scenarios where the conductor spacing in each segment is independently set show larger spatial correlation than those whose lines are not split into segments.

B. Branches

Along with the asymmetric deployment of conductors in certain types of wiring, there might be grid sections where only one of the conductors is present. For example in lighting circuits belonging to grids where monopolar wiring is deployed, branches which connect switches to the rest of the network usually include only the phase conductor. This type of branches can be seen as regular two-conductor transmission lines ended in either short or open circuit, because they leave the branch, reach the switch and come back following the same path.

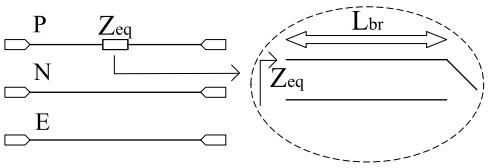

Fig. 5. Lumped element model for diversions of length L_{br} in phase conductors due to switches.

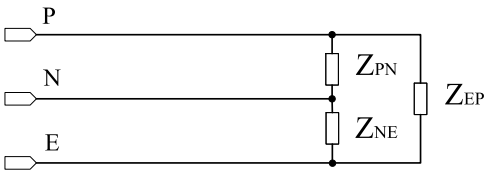

Fig. 6. Lumped element model for in-home grid ends. Each Z_{ij} impedance is modeled as a series connection of parallel RLC circuits.

In order to model these branches due to switches, we put a series load in the phase conductor whose value is taken from the input impedance of a two-conductor transmission line, see Figure 5.

C. Loads

In [4], [23] it is shown that the impedance values of many domestic appliances have a resonant characteristic in the frequency domain, thus they consist of some high-impedance peaks surrounded by large low-impedance areas. We propose a lumped element model for in-home grid ends, shown in Fig. 6, where each of the Z_{ij} loads is modeled as a series connection of parallel RLC circuits, in a similar fashion to the approach taken in [20]. During the measurement campaign we performed over an assortment of devices, it has been observed that the impedance values between pairs P-E and N-E (for the same appliance) tend to show considerable resemblance, whereas impedance values between P-N tend to display an independent behavior. In consequence, in order to design a realistic model, similar values will be assigned to loads Z_{PE} and Z_{NE}, while Z_{PN} will be set independently.

Transmitter and receiver models are depicted in Figure 3, the transmitter block is modeled as a parallel resistor between each non-transmitting pair of conductors plus a series resistor connected to one of the conductors which are attached to the signal source. The impedance value of each resistor is set to $Z_0 = 50\ \Omega$. The receiver end is instead always modeled in the same fashion regardless of the chosen signal-receiving pair: a star circuit of three resistors set to $Z_0 = 50\ \Omega$ as well.

V. The MIMO channel generator

The aforementioned MTL-based MIMO model can be used in both simple and complex PLC scenarios as there are many adjustable parameters which make this model quite versatile. However, in this section we give details of a generator configuration which has been found to fit a high variety of in-home PLC environments. For the creation of the modeling network, three steps are defined: first, the layout of the network is determined; second, every piece of transmission line is

characterized; third, loads which model the impedance of the devices attached to the power grid are added to the network. In the following, these three steps are explained.

A. Random topology generator

Since most available channel measurements correspond to small dwellings, a five sub-circuit grid will be assumed and modeled by adding five nodes to the root node. Each of the sub-circuits is modeled to obtain a realistic grid where several different paths can be found. Two kinds of sub-circuits will be considered: lighting and power sub-circuits; which differ in the wiring section and the depth of the sub-circuit itself. Lighting sub-circuit depth takes values between four and seven branches whereas for power sub-circuits it takes values between three and four. This is due to the fact that power sub-circuits are deployed to supply energy to specific groups of devices, therefore they do not reach as many wall sockets as lighting circuits do. Let us note that sub-circuit depth refers to the maximum number of series branches in a given sub-circuit and, in this case, it is related to the amount of interconnections and wall sockets in a given sub-circuit. Thus this magnitude is somehow related to the physical length of the sub-circuit, the deeper the tree the more branches it has. Although, higher sub-circuit depth does not necessarily imply lengthier wires. In this work, branch lengths are taken independently from a gamma distribution [20], $Gamma(\kappa, \theta)$, with shape parameter $\kappa = 3$ and scale parameter $\theta = 2$, which makes for a mean branch length of 6 meters. The sub-circuit creation process is summarized in Algorithm 1.

Algorithm 1 Sub-circuit generating algorithm

```
function CreateNode(Depth,Ind)
    a ← Depth ≥ MinD
    b ← Depth ≤ MaxD
    c ← U(0, Depth^{-1/2}) ≥ Thrs
    if a AND (b OR c) then                ▷ Turn node into leaf
        CreateLoad(Ind)
        return Ind
    else
        NewLine(Ind)                      ▷ Left branch
        CreateNode(Depth + 1,Ind + 1)
        NewLine(Ind)                      ▷ Right branch
        CreateNode(Depth + 1,Ind + 1)
    end if
end function
```

Let us define the variables and functions which appear in the algorithm above: $Depth$ records the depth of the current node; Ind contains the unique identifying index for each element; $MinD$ is the minimum sub-circuit depth, which is set to 3 for lighting sub-circuits and 2 for the power ones; $MaxD$ is the maximum depth, which is set to 6 for lighting sub-circuits and 4 for power sub-circuits; $U(a, b)$ returns a random variable uniformly distributed between a and b; $Thrs$ is a threshold for the random decision which manages the amount of elements in the network, it is set to 0.8; CreateLoad(Ind) is a function that transforms the given node into a load following the parameters given in Table I; and NewLine(Ind), which is a function that creates a transmission line with index Ind.

This branching strategy combines with the chosen path length distribution to generate channels whose mean path length is around 45 meters, which is a reasonable value for this type of channels.

Finally, in lighting circuits, series impedance sections are added between loads and the segment that connects it to the remainder of the sub-circuit, which correspond to the diversions in the grid due to the existence of switches. The lumped element model for switch-caused diversions comprises just a single impedance in the phase conductor whose value is equal to the input impedance of a transmission line of length L_{br} ended in either short or open circuit, according to the switch state, as shown in Figure 5.

B. Wiring settings

The goal of this section is to compute the p.u.l. parameter matrices ($\mathbf{R}$,$\mathbf{L}$,$\mathbf{C}$ and $\mathbf{G}$) for every transmission line segment. There are several approaches, analytic and experimental, for the computation of the aforementioned matrices. In this work, we will use the relations taken from [24] which have been particularized to the equal-radius conductor case:

$$\mathbf{R} = \begin{bmatrix} 2r & r \\ r & 2r \end{bmatrix} \text{ with } r = \begin{cases} \frac{1}{\sigma\pi {r_w}^2} & \text{if } r_w \leq 2\delta \\ \frac{1}{2r_w}\sqrt{\frac{\mu_0 f}{\pi\sigma}} & \text{if } r_w > 2\delta \end{cases} \tag{18}$$

$$\mathbf{L} = \begin{bmatrix} \frac{\mu_0}{\pi}\log(\frac{d_{1,0}}{r_w}) & \frac{\mu_0}{2\pi}\log(\frac{d_{1,0}d_{2,0}}{d_{1,2}r_w}) \\ \frac{\mu_0}{2\pi}\log(\frac{d_{1,0}d_{2,0}}{d_{1,2}r_w}) & \frac{\mu_0}{\pi}\log(\frac{d_{1,0}}{r_w}) \end{bmatrix} \tag{19}$$

$$\mathbf{C} = \mu_0\epsilon\mathbf{L}^{-1} \tag{20}$$

$$\mathbf{G} = 2\pi f \tan(\delta)\mathbf{C} \tag{21}$$

where r_w is the radius of the conductor, σ is its conductivity, $\log(-)$ is the natural logarithm operator, $d_{i,j}$ the distance between conductors i and j, $\tan(\delta)$ the loss angle, μ_0 the vacuum permeability, ϵ the insulator permittivity, f is the frequency for which we are computing the p.u.l. parameter matrices and δ is the penetration depth at such frequency:

$$\delta = \frac{1}{\sqrt{\pi\mu_0\sigma f}}. \tag{22}$$

Note that equations (19), (20) and (21) are obtained under two conditions. First, the insulator medium is uniform and the distance between conductors is large with respect to the conductor radius. Although our scenario does not present a uniform insulator medium, as there are discontinuities due to the wiring sheath, the conductor jacket and air; an intermediate solution can be reached by using an equivalent permittivity computed as the lineal combination of the air and the jacket permittivity, an approach previously taken in [20], given by

$$\epsilon_{eq} = x\epsilon_0 + (1 - x)\epsilon_d, \tag{23}$$

where x is the fraction of space between two given conductors filled with air, ϵ_0 is the vacuum permittivity and ϵ_d is the insulator material permittivity. For simulations, ϵ_d was set to 3. While it is true that ϵ_d varies from one type of insulator

to another, and it even changes with frequency, this choice provides a simple and reasonable value for most cases.

As for the relative closeness of the conductors, it is shown in [24] that this error is not overly restrictive as long as there is at least a one diameter separation between any pair of conductors.

The type of wiring (multipolar ribbon, multipolar symmetric and monopolar) is determined in this section. The ribbon and symmetric kinds are modeled just by setting the distances between conductors according to a certain relation. Let the phase, neutral and earth conductor be labeled as P, N and E respectively; then, the relation $d_{P,E} = d_{N,E} = 0.5d_{P,N}$ models a ribbon-wire network with the earth conductor in the middle of the wire; while $d_{P,E} = d_{N,E} = d_{P,N}$ does it for the symmetric case. Note that the p.u.l. parameter matrix expressions shown above are obtained for parallel conductors. However, home grids with monopolar cables, where the separation between conductors varies along the length of the line, do not match well with this scenario. In order to capture the variable separation between conductors, all lines are split into segments and each one of these segments is assigned its own distance triplet, obtained by following the method detailed in Algorithm 2. Being the algorithm components: $\text{EXP}(\lambda)$ returns a random variable with exponential distribution of mean λ; $MaxSep$ is a parameter which stores the maximum separation achievable between conductors in the given wire, measured in conductor diameters (typical value is 7); and $\mathbf{Y} \leftarrow \text{RANDASSIGN}(\mathbf{X})$ is a function that assigns a random permutation of the input vector $\mathbf{X}$ to the output vector $\mathbf{Y}$.

Algorithm 2 Calculate $d_{1,0}$, $d_{2,0}$ and $d_{1,2}$

$d_A \leftarrow \text{EXP}(1) + 2$
$d_B \leftarrow \text{EXP}(1) + 2$
while $d_A > MaxSep$ OR $d_B > MaxSep$ **do**
  $d_A \leftarrow \text{EXP}(1) + 2$
  $d_B \leftarrow \text{EXP}(1) + 2$
end while
$d_{max} \leftarrow \text{MIN}(d_A + d_B, MaxSep)$
$d_{min} \leftarrow \text{MAX}(\text{MAX}(d_A, d_B) - \text{MIN}(d_A, d_B), 2)$
$d_C \leftarrow \text{U}(d_{min}, d_{max})$
$[d_{P,E}, d_{N,E}, d_{P,N}] \leftarrow \text{RANDASSIGN}([d_A, d_B, d_C])$

The reason for $d_j \leftarrow \text{EXP}(1) + 2$ is that distance between conductors is measured between their centers in conductor diameters, thus the minimum distance as stated would strictly be one. Furthermore, in Section III, the expressions for the p.u.l. parameter matrix computation are accurate as long as the wire centers are separated by, at least, two conductor diameters. Moreover, exponential random variables take values in the interval $[0, +\infty)$. All this justify the necessity of adding 2 so that the mentioned conditions are not violated. It has been empirically checked that good results are achieved when using the one-mean exponential random variable, however other distributions, like Rayleigh or Gamma, could be taken into consideration as well.

C. Random load generator

To complete the channel generator, let us now characterize all network ends according to the model depicted in Figure 6. First, it must be decided the number of RLC circuits that will form each Z_{ij} impedance. Then, we determine each RLC circuit by means of the set of parameters R, f_0 and Q [20]; which are randomly obtained from the distributions shown in Table I.

Parameter	Distribution
R (Ω)	$\text{U}(2 \times 10^2, 2 \times 10^3)$
Q	$\text{U}(10, 40)$
f_0 (Hz)	$\text{EXP}(10) \times 10^6$
Number of RLC circuits	$\text{ROUND}(\text{U}(2, 7))$

TABLE I
GENERATING DISTRIBUTIONS FOR RLC PARAMETERS.

As mentioned in Section IV-C, Z_{PE} and Z_{NE} belonging to the same load are similar according to our measurements. To capture the impedance correlation between these two ports we assign their RLC circuits the same R, f_0 and Q parameters with a 5% drift. By contrast, Z_{PN} parameters are independently chosen with respect to the other port loads.

VI. VALIDATION OF THE MODEL

The objective of this section is to assess the ability of the proposed channel generator to provide statistically representative channels. To this end, a set of 120 in-home MIMO links measured in Belgium, England and Germany are compared to generated channels. The latter are obtained using the random topology generator described in Section V-A. It has been configured to yield power grids with five sub-circuits, which is the typical value found in relatively small dwellings as the measured ones. Besides this common element, measured and generated networks are unrelated. First, a qualitative analysis is accomplished. It is aimed at illustrating how the proposed model outperforms other classical bottom-up approaches, based on the sole application of the MTL theory, in reproducing the characteristics of actual channels. Next, a quantitative study is carried out to compare the characteristics of the generated 2x2 MIMO channels, and of their constituent SISO channels, to the measured ones.

Figure 7 shows the measured CFRs of the four SISO channels that form a 2x2 MIMO link established over the PN and EP ports. Similar examples can be found in [27] and [22]. As can be observed, all CFRs are different. This contrasts with the results in Figure 8, which shows the CFRs of a 2x2 MIMO link obtained from a randomly generated topology with constant distance between conductors, no diversions in the phase conductor and equal impedance values between the PN, NE and EP ports. from now on, this generator configuration will be referred to as "Plain MTL", and its resultant channels would be quite close to the ones obtained with state of the art MTL-based generators. Since the underlying physical structure is symmetric, both direct channels (PN-PN and EP-EP) and both coupled channels (PN-EP and EP-PN) have equal CFRs. In addition, the CFRs of direct and coupled channels keep a constant ratio.

It must be pointed out that the constant relation between direct and coupled channels does not mean that the parallel decomposition of the MIMO link results in just one useful

stream, since the relative attenuation between the channels also matters. To illustrate this, let us denote by $\mathbf{H}$ the channel matrix of a 2x2 MIMO link at a given frequency (for the sake of clarity, the frequency index has been omitted). Its singular value decomposition can be expressed as

$$\mathbf{H} = \begin{bmatrix} H^{11} & H^{12} \\ H^{21} & H^{22} \end{bmatrix} = \mathbf{U}\mathbf{D}\mathbf{V}^{\mathbf{H}}, \tag{24}$$

where $\mathbf{D}$ is a diagonal matrix whose elements are the singular values of $\mathbf{H}$, $\mathbf{U}$ and $\mathbf{V}$ are unitary matrices and $(-)^H$ denotes the hermitian transpose operator.

The parameter commonly used to quantify the correlation between the parallel streams in which the MIMO link is decomposed is the condition number, which for a 2x2 MIMO matrix is given by,

$$\kappa = 20\log_{10}\left(\frac{\sigma_1}{\sigma_2}\right)(dB), \tag{25}$$

where σ_i denotes the i-th singular value of $\mathbf{H}$. Without loss of generality, the first singular value is assumed to be larger than the second one. High values of κ indicate that one of the parallel streams of the MIMO link is much more attenuated than the other one. In contrast, $\kappa \to 0$ implies that almost two equal-gain streams can be obtained, which in turn may lead to a higher channel capacity than in the former case.

For illustrative purposes, let's consider a simple case with equal direct channels, $H^{11} = H^{22} = H^d$, and perfectly correlated coupled channels, $H^{12} = H^{21} = \alpha H^d$. The completely symmetric topology described above is an example of this case, where $\alpha = -1/2$. Under these circumstances, the condition number is

$$\kappa = 20\log_{10}\left(\frac{|\alpha|+1}{||\alpha|-1|}\right). \tag{26}$$

As seen, the relative attenuation between the streams of the MIMO link depends on the relative attenuation between the direct and coupled channels.

In Figure 9, it is illustrated the ability of the proposed model to generate MIMO channels with similar spatial correlation to the measured ones. It shows the CFRs of a 2x2 MIMO link generated by the proposed channel generator. As can be observed, the inclusion of asymmetric loads, irregular separation of the wires with branch segmentation and diversions in the phase conductor to the model lead to different propagation characteristics in the direct and the coupled paths, just as in actual channels.

The quantitative validation of the proposed model is accomplished by comparing results obtained with generated and measured ensembles. First, the capability of the proposed model to generate MIMO channels with similar spatial correlation to the measured one is assessed. Figure 10 shows the matrix condition number of the channels whose attenuation is depicted in Figures 7, 8 and 9.

Second, the ability of the presented model to match the characteristics of the SISO channels that comprise the MIMO link is evaluated. Figure 11 shows the average amplitude of the CFRs of the channels of the 2x2 MIMO links established over

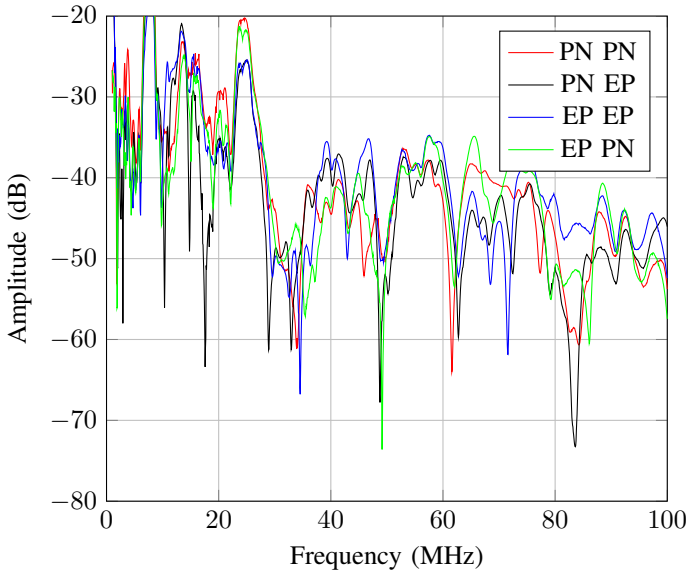

Fig. 7. Measured CFR of the SISO channels of a 2x2 MIMO link established using PN and EP ports.

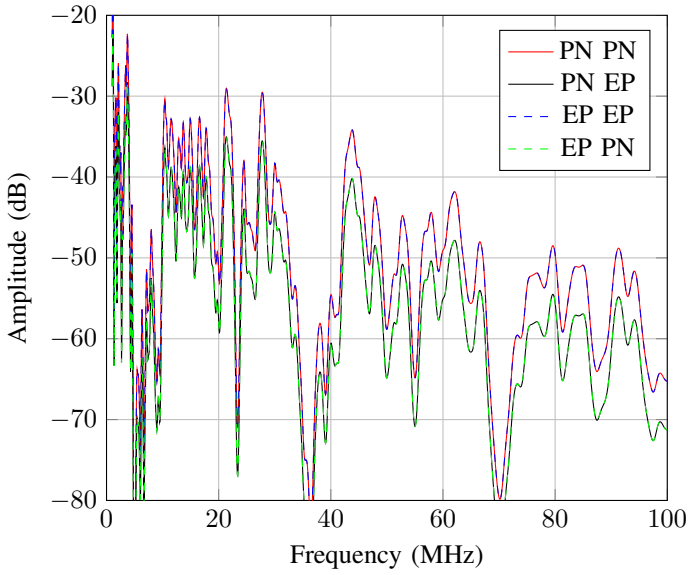

Fig. 8. CFR of the SISO channels of a 2x2 MIMO link established using PN and EP ports. They were obtained with a "Plain MTL" channel generator.

the PN and EP ports. For the sake of clarity, only the CFRs of the PN-PN and PN-EP channels are shown, but similar results have been obtained in the EP-EP and EP-PN ones. As it can be seen, there is a very good match between measured and generated curves.

Figure 12 depicts the cumulative distribution function (CDF) of the condition number of the ensemble of measured channels along with the CDF obtained from different channel generator configurations so it becomes clear the relative influence of the three innovative elements of the proposed model (cabling, branches and loads). Curve labeled as "Plain MTL", has been obtained with an MTL model excluding any of the elements proposed in the paper, i.e. varying separation between

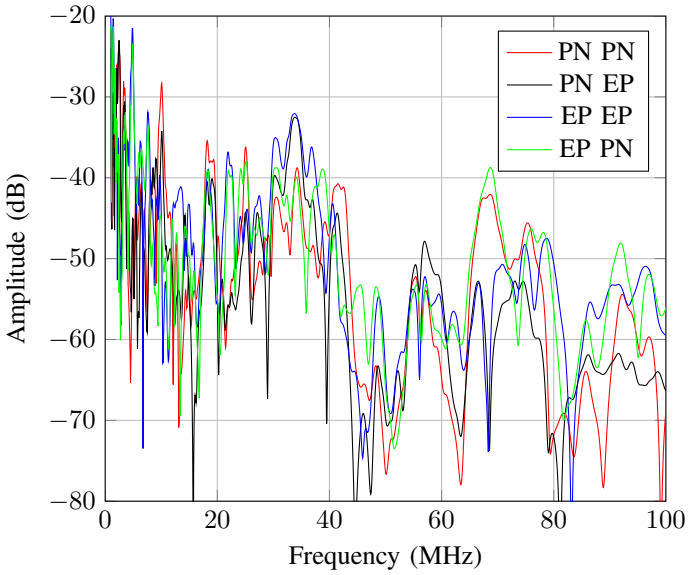

Fig. 9. CFR of the SISO channels of a 2x2 MIMO link established using PN and EP ports. They were obtained with the proposed channel generator.

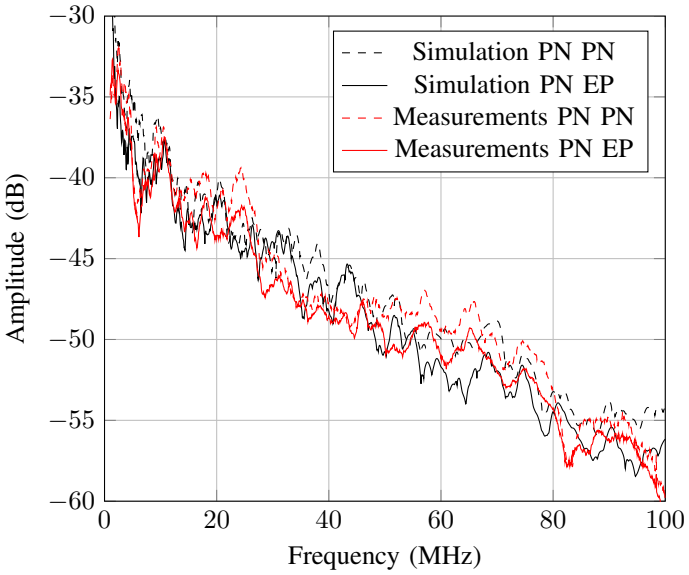

Fig. 11. Averaged amplitude of the CFRs of the SISO channels of generated and measured 2x2 MIMO links.

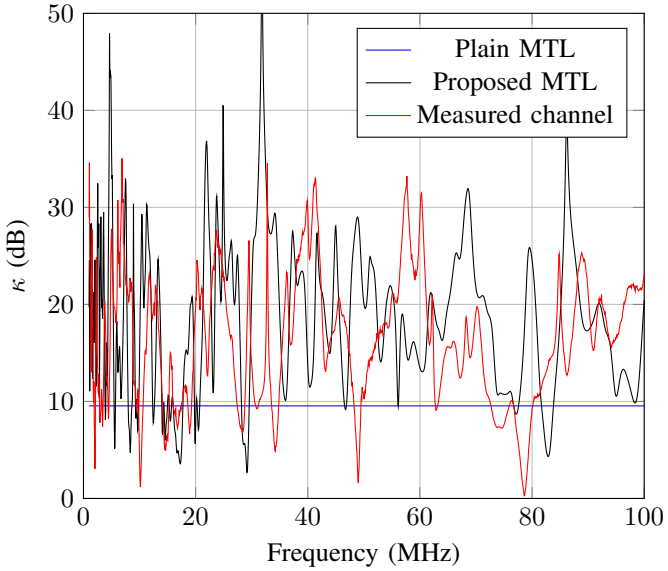

Fig. 10. Condition number of measured and generated 2x2 MIMO links.

wires, branch segmentation, diversions in the phase conductor and different loads between different ports belonging to the same socket. Hence, it essentially corresponds to an state of the art bottom-up MIMO PLC model. Since CFRs of direct and coupled paths follow the relation $H^{ij} = \alpha H^{ii}$ with $\alpha = -1/2$ at all frequencies, the condition number is constant. As shown, results are very far from the actual ones.

Curve labeled as "Plain MTL + (1)" has been obtained by including just one of the three elements: loads with different impedance values between their ports. When diversions in the phase conductor and independent interconductor distance for each branch are also included, curve denoted as "Plain MTL + (1,2,3)" results. Finally, when branch segmentation with independent interconductor distance for each segment is added to the mix, curve labeled as "proposed MTL" is obtained, which is just the proposed channel generator configuration.

As seen, the inclusion of each new element moves the simulation results towards the measured ones. The fitting to actual values is very good in almost the whole range of κ when all novel elements are incorporated to the channel generator.

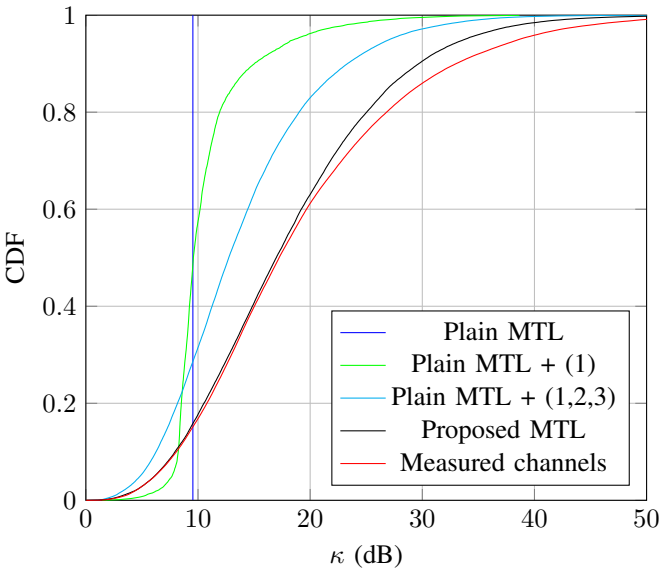

Fig. 12. CDF of the condition number of a set of measured and randomly generated 2x2 MIMO links. Plain MTL, state of the art bottom-up MIMO PLC channel models.

VII. Influence of the power grid structure in the spatial correlation

Results given in the previous section, in particular the ones in Figure 12, allow assessing the influence that some elements of indoor power grids have in the spatial correlation.

This can be useful for fitting top-down models, specially for categorizing indoor networks into classes in which the parameter that reflects the spatial correlation should be derived independently.

- *Number and type of connected devices*. The larger the number of devices, the lower the spatial correlation. This can be inferred from the comparison of the curves denoted as "Plain MTL" and "Plain MTL + (1)". The former exhibits higher correlation values and assumes that connected devices have $Z_{PN} = Z_{PE} = Z_{NE}$, which also happens when no device is plugged into a socket. Plugging a device to the grid introduces a sort of asymmetry that reduces the spatial correlation.
- *Number of light switches*. The higher the number of light switches, the lower the spatial correlation. This is suggested by curve labeled "Plain MTL + (1,2,3)", which shows lower correlation values that the "Plain MTL + (1)" one. Hence, channels established in premises with high number of rooms are expected to have lower spatial correlation values that those set up in sites with a reduced number of accommodations (assuming that each room has its own light switch).
- *Type of cables*. MIMO links established in indoor power grids in which the deployed cables have fixed distance between conductors will exhibit higher spatial correlation values. This can be inferred by noticing that curve labeled "Proposed MTL" shows lower correlation values than the one labeled "Plain MTL + (1,2,3)". Therefore, measurements acquired in networks with multipolar and unipolar cables should be placed in different categories when fitting top-down models.

VIII. Conclusion

This paper addresses the modeling of MIMO PLC channels by means of the MTL theory. It presents a statistical analysis of the spatial correlation of actual channels and shows that plain MTL-based models are unable to reflect this behavior. Three modifications are then proposed to improve this comportment: loads, branches and cabling. The first one accounts for the different impedance values measured between the ports (PN, NE and EP) of electrical devices connected to the grid. The second one includes the fact that there are grid sections where only one of the conductors is present, e.g. lighting circuit branches that connect switches to the rest of the network. The third one incorporates a variable separation that emulates the actual conductor deployment in the power grid wiring.

The proposed model leads to MIMO channels similar to the measured ones, both in terms of the characteristics of their individual SISO channels and of the correlation between them. In addition, a PLC channel generator that is able to provide statistically representative channels is given. It can be useful to evaluate the performance of transmission techniques and the design of algorithms for MIMO PLC broadband systems.

Finally, the influence of several elements of indoor power grids in the spatial correlation of MIMO channels is discussed. Provided considerations can be helpful for the fitting process of top-down models.

Acknowledgment

The authors would like to thank Marvell Hispania S.L. for its support and contribution to this work.

References

[1] *Unified high-speed wireline-based home networking transceivers - Multiple input/multiple output specification*, ITU-T Recommendation G.9963, 2011 Std.

[2] *HomePlug AV2*, HomePlug Powerline Alliance [Online] Available at: http://www.homeplug.org Std.

[3] M. Zimmermann and K. Dostert, "A Multipath Model for the Powerline Channel," *IEEE Transactions on Communications*, vol. 50, no. 4, pp. 553–559, Apr 2002.

[4] F. J. Cañete, L. Díez, J. A. Cortés, and J. T. Entrambasaguas, "Broadband Modelling of Indoor Power-Line Channels," *IEEE Transactions on Consumer Electronics*, vol. 48, no. 1, pp. 175–183, Feb 2002.

[5] A. M. Tonello, F. Versolato, B. Bejar, and S. Zazo, "A Fitting Algorithm for Random Modeling the PLC Channel," *IEEE Transactions on Power Delivery*, vol. 27, no. 3, pp. 1477–1484, 2012.

[6] M. Babic, M. Hagenau, K. Dostert, and J. Bausch, "D4: Theoretical Postulation of PLC Channel Model," Opera, Tech. Rep., 2005.

[7] J. A. Cortés, L. Díez, F. J. Cañete, and J. L. González Moreno, "On the Statistical Properties of Indoor Power Line Channels: Measurements and Models," in *IEEE International Symposium on Power Line Communications and its Applications (ISPLC)*, March 2011.

[8] M. Tlich, A. Zeddam, A. Moulin, and F. Gauthier, "Indoor Power-Line Communications Channel Characterization Up to 100 MHz-Part I: One-Parameter Deterministic Model," *IEEE Transactions on Power Delivery*, vol. 23, no. 3, p. 1392–1401, 2008.

[9] R. Hashmat, P. Pagani, A. Zeddam, and T. Chonave, "A Channel Model for Multiple Input Multiple Output in-home Power Line Networks," in *IEEE International Symposium on Power Line Communications and Its Applications*, April 2011, pp. 35–41.

[10] K. Khalil, M. Gazalet, P. Corlay, F.-X. Coudoux, and M. Gharbi, "An mimo random channel generator for indoor power-line communication," *Power Delivery, IEEE Transactions on*, vol. 29, no. 4, pp. 1561–1568, Aug 2014.

[11] A. M. Tonello and F. Versolatto, "Bottom-Up Statistical PLC Channel Modeling – Part I: Random Topology Model and Efficient Transfer Function Computation," *IEEE Transactions on Power Delivery*, vol. 26, no. 2, pp. 891–898, 2011.

[12] S. Galli and T. C. Banwell, "A Deterministic Frequency-Domain Model for the Indoor Power Line Transfer Function," *IEEE Journal on Selected Areas in Communications*, vol. 24, no. 7, pp. 1304–1316, July 2006.

[13] F. Versolatto and A. M. Tonello, "An MTL Theory Approach for the Simulation of MIMO Power-Line Communication Channels," *IEEE Transactions on Power Delivery*, vol. 26, no. 3, pp. 1710–1717, July 2011.

[14] A. M. Tonello, F. Versolatto, and A. Pittolo, "In-Home Power Line Communication Channel: Statistical Characterization," *IEEE Transactions on Communications*, vol. 62, no. 2, pp. 2096–2106, 2014.

[15] P. J. Piñero, J. A. Cortés, J. Malgosa, F. J. Cañete, P. Manzanares, and L. Díez, "Analysis and improvement of multicast communications in HomePlug AV-based in-home networks," *Elsevier Computer Networks*, vol. 62, pp. 89–100, 2014.

[16] L. Lampe and A. Vinck, "Cooperative multihop power line communications," in *Power Line Communications and Its Applications (ISPLC), 2012 16th IEEE International Symposium on*, March 2012, pp. 1–6.

[17] L. Lampe, R. Schober, and S. Yiu, "Distributed space-time coding for multihop transmission in power line communication networks," *Selected Areas in Communications, IEEE Journal on*, vol. 24, no. 7, pp. 1389–1400, July 2006.

[18] S. D'Alessandro and A. Tonello, "On rate improvements and power saving with opportunistic relaying in home power line networks," *EURASIP Journal on Advances in Signal Processing*, vol. 2012, no. 1, p. 194, 2012. [Online]. Available: http://asp.eurasipjournals.com/content/2012/1/194

[19] J. A. Cortés, F. J. Cañete, M. Toril, and L. Díez, "Feasibility Study of Power Line Communications for Last-Hop Backhaul in Small Cell Deployment," Vodafone Group, Tech. Rep. Contract 806/59.3785, 2012.

[20] F. J. Cañete, J. A. Cortés, L. Díez, and J. T. Entrambasaguas, "A Channel Model Proposal for Indoor Power Line Communications," *IEEE Communications Magazine*, vol. 49, no. 12, pp. 166–174, December 2011.

[21] ETSI, "PowerLine Telecommunications (PLT). MIMO PLT. Part 3: Setup and Statistical Results of MIMO PLT Channel and Noise Measurements," *TR 101 562-3 V1.1.1 (2012-02)*, 2012.
[22] L. T. Berger, A. Schwager, P. Pagani, and D. Schneider, *MIMO Power Line Communications: Narrow and Broadband Standards, EMC, and Advanced Processing*. CRC Press, 2014.
[23] M. Antoniali and A. M. Tonello, "Measurement and Characterization of Load Impedances in Home Power Line Grids," *IEEE Transactions on Instrumentation and Measurement*, vol. 63, no. 3, pp. 548–556, March 2014.
[24] C. R. Paul, *Analysis of Multiconductor Transmission Lines*. Wiley, 1994.
[25] J.-J. Werner, "The HDSL environment [high bit rate digital subscriber line]," *Selected Areas in Communications, IEEE Journal on*, vol. 9, no. 6, pp. 785–800, Aug 1991.
[26] F. Versolatto and A. M. Tonello, "A MIMO PLC Random Channel Generator and Capacity Analysis," in *IEEE International Symposium on Power Line Communications and Its Applications*, April 2011, pp. 66–71.
[27] D. Schneider, A. Schwager, W. Baschlin, and P. Pagani, "European MIMO PLC Field Measurements: Channel Analysis," in *IEEE International Symposium on Power Line Communications and Its Applications*, March 2012, pp. 304–309.

Julio A. Corchado received the Telecommunication Engineering degree from the University of Málaga (UMA), Spain, in 2014. In 2014, he joined the Communication Engineering Department, University of Málaga, as an associate researcher where he is currently working toward the Ph.D. degree. His research interests include digital signal processing for communications and power-line communication, the latter mainly focused on channel modeling.

José A. Cortés received the M.S. and Ph.D. degrees in telecommunication engineering in 1998 and 2007, respectively, from the University of Málaga (Spain). In 1999 he worked for Alcatel España R&D. This same year he joined the Communication Engineering Department of the University of Málaga, where he became an Associate Professor in 2010. From 2000 to 2002 he collaborated with the Nokia System Competence Team in Málaga. He is the coauthor of the Best paper award at the IEEE International Symposium on Power Line Communications (ISPLC) 2012. Since 2013 he is on a leave on absence and works as a consultant. As such, he is collaborating on the development of Atmel's power line communications (PLC) solutions. He served as TPC Co-Chair of the IEEE ISPLC 2014. His research interests include digital signal processing for communications, mainly focused on channel characterization and transmission techniques for power line communications (PLC).

Francisco J. Cañete received the M.S. and Ph.D. degrees in Telecommunication Engineering in 1996 and 2004, respectively, from the Universidad de Málaga (Spain). In 1996, he worked for the Instrument and Control Department at INITEC (Empresa Nacional de Ingeniería y Tecnología) in the design of power plants. In 1997, he worked for Alcatel España R&D Department in the design of Wireless Local Loop systems. In 1998, he joined the Ingeniería de Comunicaciones Department at Universidad de Málaga and, at present, he is an Associate Professor.. From 2000 to 2001, he collaborated with the Nokia System Competence Team in Málaga in the design of Radio Access Networks. His current research activity is focused on signal processing for digital communications with special interest in channel modeling and transmission techniques for wireless systems, underwater acoustic communications and Power-Line Communications.

Luis Díez received the M.S. and Ph.D degrees from Polytechnic University of Madrid, Spain, in 1989 and 1995 respectively, both in telecommunications engineering. From 1987 to 1997 he has been with the Department of Signals, Systems and Radiocommunication, Polytechnic University of Madrid, where he was assistant professor. Since 1997 he has been with the Department of Communications Engineering, University of Málaga, where he is now associate professor. His research interests is primarily digital communication, a field in which he has work for many years. His experience include most of its application: voiceband, DSL and cable modems; satellite, mobile and power line communications, etc. and technical aspects: synchronization, adaptive signal processing, modulation, coding and multiple access.